Int J Clin Exp Pathol 2016;9(6):6371-6377
www.ijcep.com /ISSN:1936-2625/IJCEP0025426

Original Article

Identification of the eEF1A2 expression level by RNA-seq analysis in doxorubicin-tolerant K562 cell lines

Xiaoye Zhang[1*], Liang Zou[2*], Dan Yu[2], Ting Zhang[2], Weiqi Yao[3,4], Bing Yuan[3], Wei Xiong[3], Dongcheng Wu[1,3], Hui Cheng[2]

[1]School of Basic Medical Science, Wuhan University, Wuhan 430072, Hubei, China; [2]Department of Hematology, Wuhan Integrated TCM & Western Medicine Hospital, Wuhan 430022, Hubei, China; [3]Department of Research, Wuhan Hamilton Biotechnology-Co., LTD., Wuhan 430075, Hubei, China; [4]Department of Oncology, Renmin Hospital of Wuhan University, Wuhan 430060, Hubei, China. [*]Co-first authors.

Received February 1, 2016; Accepted April 26, 2016; Epub June 1, 2016; Published June 15, 2016

Abstract: Myeloid neoplasms are broadly divided into acute myeloid leukemia (AML) and chronic myeloid disorders. Understanding the molecular mechanisms of myeloid neoplasms is required to develop the novel therapeutic target for the diseases. In this study, about 22 million sequencing reads were achieved from the K562 control and other three drug-tolerant cell lines which were treated with different concentrations of doxorubicin to screen the changes of gene expression. The gene expression profiles in three groups, namely K-K1, K-K3 and K-K5, were independently analyzed, followed by series cluster analysis for these groups. The clusters were classified into 26 profiles according to the differential gene expressions. GO and KEGG pathway analysis were then performed to establish the gene expression profiles separately. A gene of interest, termed eEF1A2, was found to be upregulated in the K562 cell lines as the final concentrations of doxorubicin increased, which indicated that eEF1A2 could be a novel target for the treatment of CML.

Keywords: RNA-Seq, eEF1A2, K562, CML, doxorubicin-tolerant

Introduction

Myeloid neoplasms, a type of hematologic malignancies of the blood-forming system, are broadly divided into acute myeloid leukemia (AML) and chronic myeloid disorders according to the percentage of bone marrow (BM) infiltration by immature blasts [1]. The criterion cut-off for AML is defined by 20% and more infiltrating immature blasts. Chronic myeloid disorders such as chronic myeloid leukemia (CML) can evolve over time into AML [2].

CML, a heterogeneous disease with an incidence of 1-2 cases per 100,000 people for all age groups [3], is caused by a translocation of the Abelson oncogene (ABL) on chromosome 9 and the breakpoint cluster region (BCR) gene on chromosome 22 [4]. CML is characterized by the overproduction and accumulation of CD5+ monoclonal B lymphocytes in peripheral blood, bone marrow and secondary lymphoid organs [5]. The progressive expansion of CML clone occurs in specific niches within the lymphoid tissues and bone marrow, where CML cells are protected from apoptosis. The imbalance between cell death and proliferation will ultimately lead to occurrence and development of the disease. Without effective treatment, chronic phase CML inevitably evolves via an accelerated phase into blast crisis [6], a stage at which the disease becomes highly resistant to any treatment provided. The blasts in two thirds of CML cases, whose phenotype is similar to t of AML, are of myeloid origin.

Remarkable progress has been achieved in the treatment of myeloid neoplasms with the application of chemoimmunotherapy regimens. The specific tyrosine kinase inhibitor (TKI), one of the most commonly used options, demonstrates long-term disease control and good tolerability [7]. TKI has become a gold standard in CML therapy since its introduction into clinics in 2001 [8]. However, myeloid neoplasms remains to be an incurable disease due to its significant relapse rate or resistance to conventional therapy [9], which mainly results from the dysregulation of specific transporters that protect the neoplastic cells from harmful molecules. There

Table 1. Summary of statistical analysis of RNA-Seq data in this study

	K562	K562/0.01	K562/0.03	K562/0.05
Total Reads number	18136152	17995434	19189643	16758591
Reads mapped to reference genome	16626445	16457671	17502650	15357171
Mapped reads ratio (%)	91.7	91.5	91.2	91.6
Total Unique Mapped reads number	15902799	15726155	16703555	14674523
Unique Mapped Ratio (%)	87.7	87.4	87	87.6

Table 2. The primer used in the qPCR and RT-PCR

Gene	Forward (5'-3')	Reverse (5'-3')
GAPDH*	CATGAGAAGTATGACAACAGCCT	AGTCCTTCCACGATACCAAAGT
eEF1A2	TGCACCACGAGGCTCTGA	TGCTGTCCCCACACACGTT
FXII	AGCTTGGAGTCAACACTTTCG	AACGACTGTGTGCTCTTCAGC

*GAPDH was used as the internal control.

is an urgent need to investigate the mechanisms underlying the initiation and development of myeloid neoplasms and it resistance to chemoimmunotherapy, which may help to identify novel targets and establish effective regimens.

Since the genetic classification and molecular mechanisms of myeloid neoplasms have not been clarified yet, it may be practical and more efficient to use sequencing techniques such as high-throughput RNA-sequencing (RNA-Seq), a powerful and cost-efficient tool for transcriptome analysis, to detect gene specific expressions, gene fusions, non-coding transcripts and possibly the alternative splicing variants [9] for myeloid neoplasms.

Doxorubicin, also called adriamycin, is one of the most wide-spectrum antineoplastics and potent first-line chemotherapeutic anticancer drugs because of its high efficacy and tolerance. In this study, a couple of chronic myeloid leukemic K562 cell lines treated with different concentrations of doxorubicin were analyzed in parallel, and a striking upregulation of the transcript level of eukaryotic translation elongation factor 1 alpha 2 (eEF1A2) was clearly observed as the concentrations of doxorubicin increased, which indicated that FXII might be responsible to the drug-tolerance in CML.

Materials and methods

Establishment of drug-tolerant cell lines

Chronic myeloid leukemic K562 cell lines were cultured in Dulbecco's Modified Eagle's Medium (DMEM) medium supplemented with 10% fetal bovine serum in an atmosphere of 5% CO_2 at 37°C. K562 cells were treated with doxorubicin at serial concentrations of 0.01 mg/L, 0.03 mg/L, and 0.05 mg/L and the stable drug-tolerant cell lines were then established, named as K562/0.01, K562/0.03 and K562/0.05, respectively.

cDNA synthesis

The K562 cells were collected and total RNA was extracted using Trizol reagent (Promega) according to the manufacturer's protocol. Total RNA was resuspended in 40 μl of nuclease-free water and its concentration was measured through NanoDrop 2000 (Thermo Scientific NanoDrop 2000). After the quantity and quality of RNA were determined, 2 μg of total RNA was used as templates to synthesize the first-strand cDNA using an M-MLV Reverse Transcriptase kit (Promega).

Bioinformatic analysis

Quality control was done and raw data was filtered by software Fast-QC. Clean and high-quality sequencing reads were aligned against transcript references using Bowtie 2.0.0 [11]. Mapsplice was used to align RNA-Seq reads. GO and KEGG pathway analysis were performed on the web tool DAVID based on the differential gene expression levels [12].

To identify differentially expressed genes (DEGs) among K562 control cells and other drug treated cell lines, the false discovery rate (FDR) method was used to determine the threshold of *P*-value in multiple tests [13, 14]. A FDR≤0.001 and an absolute value of the log2 ratio≥1 were considered as statistically significant in gene transcriptomes among four different cell lines. Functional annotation was applied to enrich genetic annotation from K562

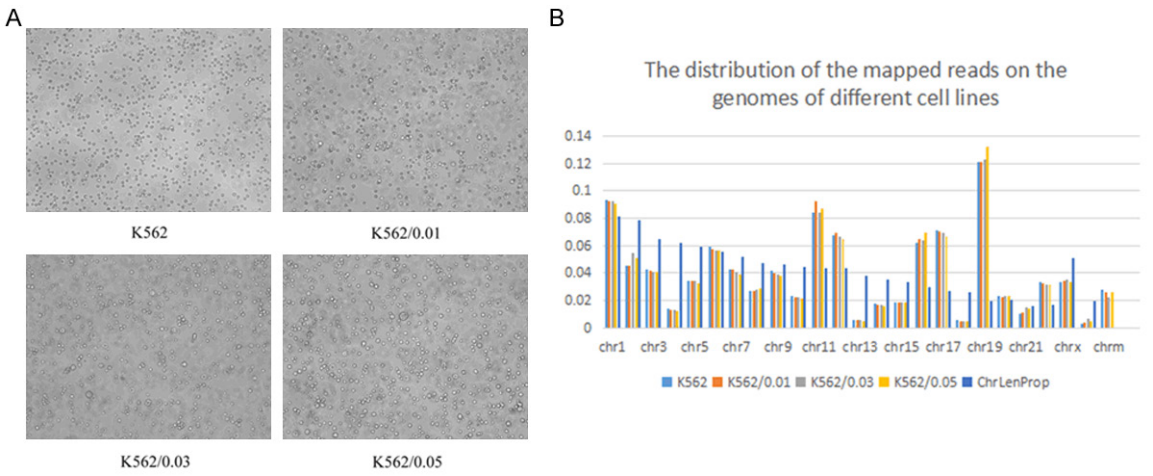

Figure 1. The distribution of the mapped reads on the genomes in different cell lines. Reads distribution was shown on each chromosome of the genome in different cell lines, including K562, K562/0.01, K562/0.03, K562/0.05, and cells from a normal person. The distribution value was calculated by the number of mapped reads in a specific exon divided by the number of reads in all exons.

control and other three cell lines. The *P*-value for significant overpresentation of a particular GO or pathway category was calculated by the hypergeometric distribution.

Quantitative real-time PCR and reverse transcription PCR

Unigenes of interest were subjected to quantitative real-time PCR (qRT-PCR) analysis. Primers were designed based on the matched region between the unigenes and the known genes in the KEGG database. These primers are shown in **Table 2**. PCR was performed as follows: 1 μl (10 μM) of each primer, 10 μl of SYBR® qPCR Mix (TOYOBO), and 200 ng of cDNA as template in a final total volume of 20 μl. The cycling parameters were 95°C for 4 min followed by 95°C for 15 s, 55°C for 15 s and 72°C for 20 s, 45 cycles. Triplicate of real-time PCR reaction was performed for each gene tested. The GADPH gene (Unigene27520_All, 100% similarity) was used as the internal control gene [15]. Relative level of gene expression was analyzed by the $2^{-\Delta\Delta CT}$ method [16]. Reverse transcription PCR (RT-PCR) was performed on a Bio-Rad T100™ Thermal Cycler. The cycling parameters were as follows: 95°C for 4 min, followed by 30 cycles of 95°C for 10 s, 55°C for 10 s, 72°C for 10 s, and a final extension of 72°C for 10 min. PCR products were analyzed on 1.0% agarose gel electrophoresis.

Results

RNA-Seq and transcriptome overview

In this study, we established four cDNA libraries K562, K562-1, K562-3 and K562-5 from normal K562 cells and drug-tolerant K562/0.01, K562/0.03 and K562/0.05 cell lines, respectively (**Figure 1A**). The RNA-Seq generated transcriptomic raw reads ranging from 19,787,363 to 22,474,891 for each library. Moreover, sequencing reads matched to 28S, 18S rRNA and mitochondrial transcripts were removed to eliminate the non-nuclear transcripts, and only the clean reads were used for further analyses. The mapping rates were 91.7%, 91.5%, 91.2%, and 91.6% for K562/0.01, K562/0.03 and K562/0.05 cell lines, respectively. The density of the matched reads on different regions of the genome was shown in **Figure 1B**. More detailed information was summarized in **Table 1**.

Functional analysis of differential gene transcriptions among three paired groups of K562 cells

In this study, the control cell line and experimental ones were divided into three groups K562 with K562-1, K562 and K562-3 and K562 and K562-5, which were initialized as K-K1, K-K3 and K-K5 respectively. These groups were analyzed separately and series

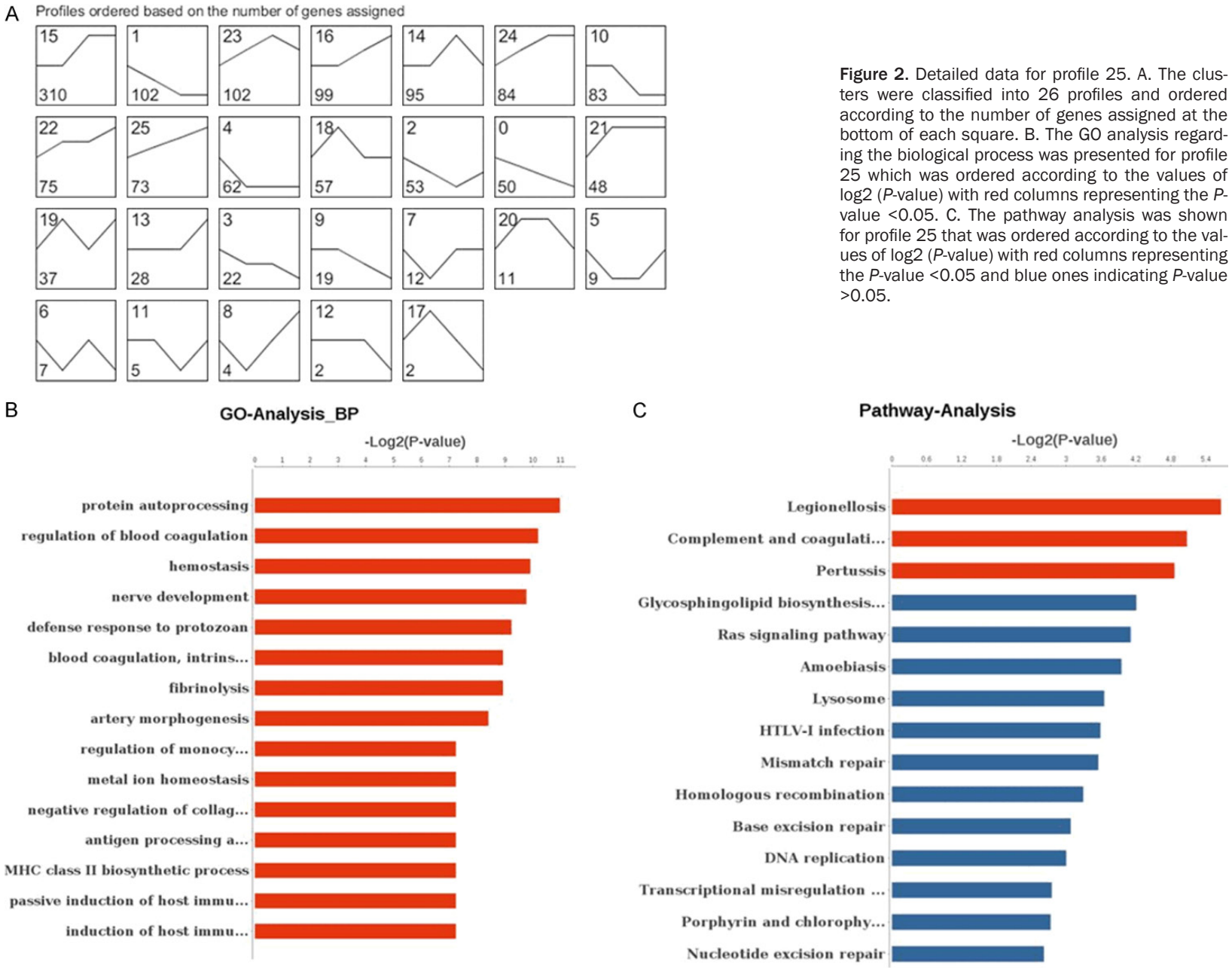

Figure 2. Detailed data for profile 25. A. The clusters were classified into 26 profiles and ordered according to the number of genes assigned at the bottom of each square. B. The GO analysis regarding the biological process was presented for profile 25 which was ordered according to the values of log2 (*P*-value) with red columns representing the *P*-value <0.05. C. The pathway analysis was shown for profile 25 that was ordered according to the values of log2 (*P*-value) with red columns representing the *P*-value <0.05 and blue ones indicating *P*-value >0.05.

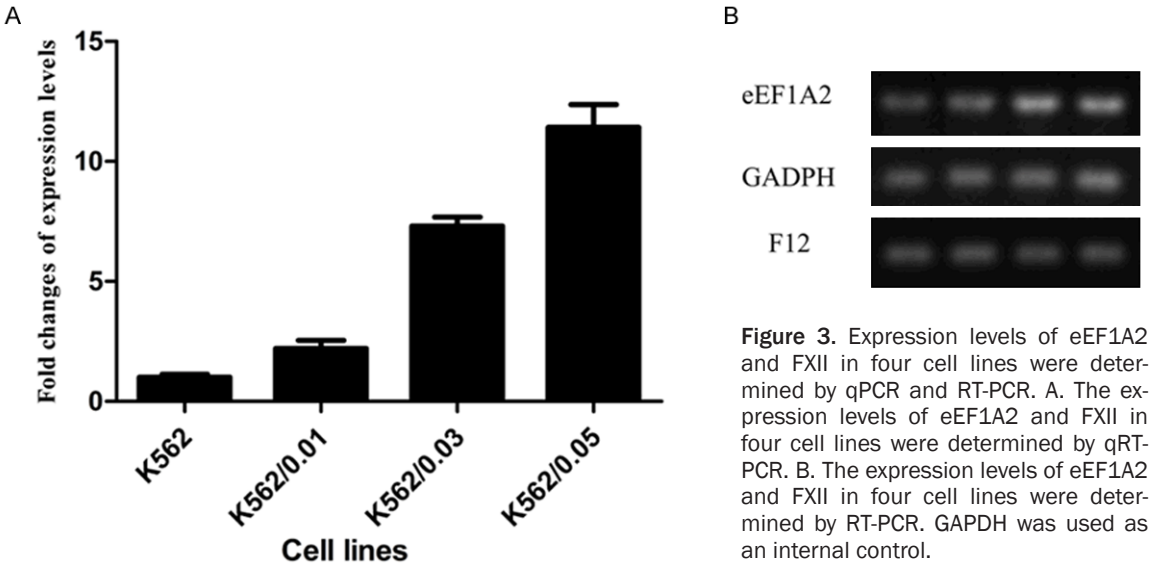

Figure 3. Expression levels of eEF1A2 and FXII in four cell lines were determined by qPCR and RT-PCR. A. The expression levels of eEF1A2 and FXII in four cell lines were determined by qRT-PCR. B. The expression levels of eEF1A2 and FXII in four cell lines were determined by RT-PCR. GAPDH was used as an internal control.

cluster analysis was done to find the union of sets among those three groups. Twenty-six profiles of the clusters were classified according to the differential changes of protein expression. As observed, 73 genes were upregulated in profile 25 and 50 genes were downregulated in profile 0 as the final concentration of doxorubicin increased from 0 to 0.05 mg/L (**Figure 2A**).

Gene ontology (GO) analysis was performed to unify the representation of gene functions, including biological process (16,164 sequences), cellular component (17,457 sequences), and molecular function (15,893 sequences). Results of GO analysis were also classified into 26 profiles as previously described, and the GO-analysis about biological process in profile 25 was shown in **Figure 2B**. GO enrichment showed that there were 169 GO terms with *P*-value <0.05 in biological process, and KEGG (Kyoto Encyclopedia of Genes and Genomes) pathway analysis indicated that 3 pathway terms in profile 25 with *P*-value <0.05 were indicated with red columns (**Figure 2C**).

Real-time PCR validation of differential gene transcriptions

To confirm the reliability and accuracy of the RNA-Seq transcriptome data, the expression level of the selected gene eEF1A2 (eukaryotic translation elongation factors 1 alpha 2) was further quantified using qRT-PCR and RT-PCR. The results nicely reproduced the RNA-Seq data. These data suggested that the RNA-Seq was able to reliably reveal the changes of transcript levels in K562 and drug-tolerant cell lines (**Figure 3A**, **3B**).

Discussion

Transcriptome changes are directly related to the changes of protein expression, which are likely associated with tumor development and drug-tolerance. Therefore, we screened a whole genome transcriptome by RNA-Seq to see transcriptome changes in the drug-tolerance in CML, hence to determine the genes that may be involved in specific biological process. In our study, we sequenced the transcripts from four cell lines of K562 that were cultured in the presence of different concentrations of doxorubicin, which induced complex changes of transcripts in different cell lines of CML. The clusters were classified into 26 profiles among which 50 genes were downregulated in profile 0 while 73 genes were upregulated in profile 25 as the final concentration of doxorubicin in the media increased from 0 to 0.05 mg/L. GO and KEGG pathway analysis for the differential gene expressions revealed that these genes were mainly associated with protein autoprocessing, blood coagulation, homeostasis, and nerve development.

eEF1A is one of the four subunits that constitute the eukaryotic elongation factor 1. This protein includes two isoforms namely eEF1A1 and eEF1A2. The eEF1A2 has been considered as an oncogene marker because it is highly

expressed in a subset of cancers, such as ovarian cancer [17], breast cancer [18], and pancreatic cancer [19]. This isoform is involved in a variety of biological processes including targeting proteins for degradation [20], heat shock response [21], apoptosis [22], and phosphatidylinositol signaling [23]. The roles of eEF1A, especially protein eEF1A2, in both CML and drug-tolerance remain unclear. In this study, we showed evidence that eEF1A2 did express in K562 cell line, and the expression was up-regulated as the concentration of doxorubicin increased, which indicated that eEF1A2 may be involved in the establishment of drug-tolerance in CML.

eEF1A2 is able to activate the phospholipid, JAK/STAT, and Akt pathways, which have been extensively shown to be involved in the cellular transformation and oncogenesis in tumors such as breast cancer. This led us to hypothesize that the eEF1A2 protein might play a role in the drug-tolerance in CML via activating the phospholipid, JAK/STAT, or Akt pathways. Further studies are needed to test this hypothesis.

In recent years, Thomas Renné found that FXII targets thrombosis without any impact on hemostasis and exerts mitogenic activity with implications for angiogenesis independent of its protease activity in vivo [24, 25]. In our study, RNA-Seq data showed that FXII was upregulated as the concentrations of doxorubicin increased from 0 to 0.05 mg/L in different cell lines of K562. RT-PCR and qPCR experiments confirmed that eEF1A2 was strikingly upregulated when the cell line K562 was treated with doxorubicin, while FXII expression levels had no significant difference among the different concentrations of drug treated (**Figure 3B**). More studies are needed to investigate whether FXII is involved in the establishment of drug-tolerance in CML.

Doxorubicin has now been widely used to treat different type of solid and hematopoietic cancers such as breast cancer, osteosarcomas, acute myeloid leukemia, and leukemias, however, the response rate and overall survival after treatment in some cases remained unsatisfactory [26, 27]. Although our RNA-Seq data are helpful for our future experimental design, more studies are absolutely needed in order to find the potential novel targets and treatments for doxorubicin-resistant tumors.

Disclosure of conflict of interest

None.

Address correspondence to: Dongcheng Wu, School of Basic Medical Science, Wuhan University, Wuhan 430072, Hubei, China. E-mail: biozhang@foxmail.com; Hui Cheng, Department of Hematology, Wuhan Integrated TCM & Western Medicine Hospital, Wuhan 430022, Hubei, China. E-mail: baby_1229@qq.com

References

[1] Swerdlow SH, Campo E, Harris NL, Jaffe ES, Pileri SA, Stein H. WHO Classification of Tumours of Haemopoietic and Lymphoid Tissues. Lyon: IARC Press; 2008.
[2] Tefferi A. Overview of the Myeloproliferative Neoplasms. Up To Date: Waltham, MA: 2013.
[3] Jemal A, Siegel R, Xu J, Ward E. Cancer statistics, 2010. CA Cancer J Clin 2010; 60: 277-300.
[4] Payandeh M, Sadeghi M, Sadeghi E. Treatment and Survival in Patients with Chronic Myeloid Leukemia in a Chronic Phase in West Iran. Asian Pac J Cancer Prev 2015; 16: 7555-9.
[5] Kavalerchik E, Goff D, Jamieson CH. Chronic myeloid leukemia stem cells. J Clin Oncol 2008; 26: 2911-510.
[6] Perrotti D, Jamieson C, Goldman J, Skorski T. Chronic myeloid leukemia: mechanisms of blastic transformation. J Clin Invest 2010; 120: 2254-64.
[7] Wong S, Witte ON. The BCR-ABL story: bench to bedside and back. Annu Rev Immunol 2004; 22: 247-30610.
[8] O'Brien SG, Guilhot F, Larson RA, Gathmann I, Baccarani M, Cervantes F, Cornelissen JJ, Fischer T, Hochhaus A, Hughes T, Lechner K, Nielsen JL, Rousselot P, Reiffers J, Saglio G, Shepherd J, Simonsson B, Gratwohl A, Goldman JM, Kantarjian H, Taylor K, Verhoef G, Bolton AE, Capdeville R, Druker BJ; IRIS Investigators. Imatinib compared with interferon and low-dose cytarabine for newly diagnosed chronic-phase chronic myeloid leukemia. N Engl J Med 2003; 348: 994-100410.
[9] Zahreddine H, Borden KL. Mechanisms and insights into drug resistance in cancer. Front Pharmacol 2013; 4: 28.
[10] Wang Z, Gerstein M, Snyder M. RNA-Seq: a revolutionary tool for transcriptomics. Nat Rev Genet 2009; 10: 57-63.
[11] Langmead B, Trapnell C, Pop M, Salzberg SL. Ultrafast and memory-effcient alignment of short DNA sequences to the human genome. Genome Biol 2009; 10: R25.
[12] Huang da W, Sherman BT, Lempicki RA. Systematic and integrative analysis of large

gene lists using DAVID bioinformatics resources. Nat Protoc 2009; 4: 44-57.
[13] Audic S, Claverie JM. The significance of digital gene expression profiles. Genome Res 1997; 7: 986-995.
[14] Benjamini Y, Drai D, Elmer G, Kafkafi N, Golani I. Controlling the false discovery rate in behavior genetics research. Behav Brain Res 2001; 125: 279-284.
[15] Xiong W, Yang J, Wang M, Wang H, Rao Z, Zhong C, Xin X, Mo L, Yu S, Shen C, Zheng C. Vinexin β Interacts with Hepatitis C Virus NS5A, Modulating Its Hyperphosphorylation To Regulate Viral Propagation. J Virol 2015; 89: 7385-400.
[16] Livak KJ, Schmittgen TD. Analysis of relative gene expression data using real-time quantitative PCR and the 2(-delta delta C(T)) method. Methods 2001; 25: 402-408.
[17] Anand N, Murthy S, Amann G, Wernick M, Porter LA, Cukier IH, Collins C, Gray JW, Diebold J, Demetrick DJ, Lee JM. Protein elongation factor EEF1A2 is a putative oncogene in ovarian cancer. Nat Genet 2002; 31: 301-5.
[18] Tomlinson VA, Newbery HJ, Wray NR, Jackson J, Larionov A, Miller WR, Dixon JM, Abbott CM. Abbott CM: Translation elongation factor eEF1A2 is a potential oncoprotein that is overexpressed in two-thirds of breast tumours. BMC Cancer 2005; 5: 113.
[19] Chao X, Duan-min H, Zhu Q. EEF1A2 promotes cell migration, invasion and metastasis in pancreatic cancer by upregulating MMP-9 expression through Akt activation. Clin Exp Metastasis 2013; 30: 933-44.
[20] Chung CM, Man C, Jin Y, Jin C, Guan XY, Wang Q, Wan TS, Cheung AL, Tsao SW. Amplification and overexpression of aurora kinase A (AURKA) in immortalized human ovarian epithelial (HOSE) cells. Mol Carcinog 2005; 43: 165-74.
[21] Shamovsky I, Ivannikov M, Kandel ES, Gershon D, Nudler E. RNA-mediated response to heat shock in mammalian cells. Nature 2006; 440: 556-60.
[22] Chang R, Wang E. Mouse translation elongation factor eEF1A-2 interacts with Prdx-I to protect cells against apoptotic death induced by oxidative stress. J Cell Biochem 2007; 100: 267-78.
[23] Amiri A, Noei F, Jeganathan S, Kulkarni G, Pinke DE, Lee JM. eEF1A2 activates Akt and stimulates Akt-dependent actin remodelling, invasion and migration. Oncogene 2007; 26: 3027-40.
[24] Kenne E, Renné T. Factor XII: a drug target for safe interference with thrombosis and inflammation. Drug Discov Today 2014; 19: 1459-64.
[25] Renné T, Schmaier AH, Nickel KF, Blombäck M, Maas C. In vivo roles of factor XII. Blood 2012; 120: 4296-303.
[26] Ishikawa T. Future perspectives on the treatment of hepatocellular carcinoma with cisplatin. World J Hepatol 2009; 1: 8-16.
[27] Kunjachan S, Rychlik B, Storm G, Kiessling F, Lammers T. Multidrug resistance: Physiological principles and nanomedical solutions. Adv Drug Deliv Rev 2013; 65: 1852-1865.